

Original Article

Investigation of optical properties of sodium superoxide loaded polyaniline in uv and visible region

Rajesh Barde^{1*}, Kailash Nemade², and Sandeep Waghuley³¹ Department of Physics, Government Vidarbha Institute of Science and Humanities, Amravati, 444604 India² Department of Physics, Indira Mahavidyalaya, Kalamb, India³ Department of Physics, Sant Gadge Baba Amravati University, Amravati 444602, India

Received: 5 November 2021; Revised: 19 January 2022; Accepted: 30 October 2022

Abstract

The PANi/NaO₂ composites were prepared using an ex-situ technique in 5–20 wt.% range. The NaO₂ was prepared in a single step by heating sodium nitrate in oxygen rich environment. Ultraviolet-visible spectroscopy was employed to extract optical parameters like direct band gap, refractive index, complex dielectric constant and optical conductivity. The refractive index increased with NaO₂ content for 5 and 10 wt. %, and then decreased possibly due to non-bridging oxygen (NBO) atoms. The composite with 10 wt. % NaO₂ showed the largest refractive index. On increasing the concentration of NaO₂, the band gap decreased from 2.538 to 2.307 eV and became narrower. Beyond 225 nm wavelength the extinction coefficient increased linearly, indicating that light trapping was proportional to wavelength. Both parts of the dielectrics follow the same pattern and the real dielectric constant is higher than the imaginary dielectric constant. The optical conductivity increased with $h\nu$ due to a change in density of localized states in the band gap, and also possibly due to the electrons excited by photon energy.

Keywords: chemical synthesis, sodium superoxide, optical conductivity, direct band gap, dielectric constant

1. Introduction

Conducting polymers are pursued with a view to applications. With long-conjugated structures, these polymers have exclusive properties such as flexibility, thermal and electrical stability, ease of synthesis, and durability (Cabuka & Gunduz, 2017). With the help of a series of simple anionic or cationic species, the conductivity of such polymers is approached through chemical oxidation or reduction reactions (Chen, 2003). The conducting polymers behave like semiconductors with small charge carrier mobility, and their conductivity approaches the range of metals on doping with suitable dopants (Khairy, & Gouda, 2015). The transport, optical and mechanical properties of these polymers can

changed with the addition of dopant agents (Vadukumpully, Paul, Mahanta, & Valiyaveetil, 2011). The most common conducting polymer is polyaniline (PANi) because it is environmentally stable, easy to synthesize, has variable conductivity, and remarkable chemical, electrical and optical properties (Mini, Archana, Raghunath, Sharanappa, & Devendrappa, 2016). It has industrial applications in electrochromic devices, sensors, conductive paints, drug delivery, rechargeable battery electrolytes, and solar cells (Stenicka *et al.*, 2008; Yilmaz, Akgoz, Cabuk, & Karaagac., 2011). The PANi can be synthesized from acidic aqueous solutions chemically or electrochemically. The chemical method is useful for large scale production of PANi, as it is very affordable. Oxidative polymerization is widely used for the preparation of PANi with an oxidant like ammonium persulfate ((NH₄)₂S₂O₈) (Mathew, Yang, & Mattes, 2002).

Nowadays, sodium-ion batteries appear to be most promising for electrical energy storage, to address the energy crisis and the pollution from fossil fuels (Li *et al.*, 2019; Xu,

*Corresponding author

Email address: rajeshbarde1976@gmail.com

Hui, Dinh, Hui, & Wang, 2019). The NaO₂ battery that takes advantage of superoxide chemistry differentiates itself from current energy-storage techniques (Ren, & Wu, 2013). Sodium superoxide has more feasible cell chemistry than lithium oxide, due to the discharge products (Hartmann *et al.*, 2013). The preparation of stable superoxide is a complicated task for researchers. Nemade *et al.* reported a novel synthesis approach for stable NaO₂. The nanoparticles of NaO₂ are synthesized by spray pyrolysis while maintaining high-density oxygen environment, so that a higher purity of the superoxide phase is achieved. These batteries can be cycled forming sodium superoxide as the lone discharge product with improved cycle life (He *et al.*, 2016). Peled *et al.* reported that on using sodium as the anode and oxygen as the cathode, these batteries ran several cycles at the temperature of 105°C (Peled, Golodnitsky, Mazor, Goor, & Avshalomov, 2011). The 0.2 V charge polarization of sodium superoxide battery makes it a potential competitor to lithium-oxygen batteries. These results show the formation of NaO₂ crystals in a one-electron allocation step as a solid discharge. This suggests replacing lithium-ions by sodium in batteries, with an unexpected outcome of metal-air batteries (Hartmann *et al.*, 2013). These batteries have garnered lots of attention because they exhibit the highest theoretical energy density and also offer the benefits of using abundant rare earth elements and potential cost efficiency (Park *et al.*, 2018).

In this study, we plan to examine the optical properties of NaO₂ doped polyaniline in UV and visible regions at room temperature. Several parameters like band gap, refractive index, complex dielectric constant, and optical conductivity were investigated.

2. Materials and Methods

2.1 Materials

AR grade chemicals (99% purity, SD Fine) were used to prepare PANi/NaO₂ Composites. Sodium nitrate was used for the synthesis of sodium superoxide (NaO₂). For the synthesis of polyaniline (PANi) aniline monomer and ammonium persulfate was used. As such synthesized PANi was washed with hydrochloric acid. Doubled distilled (De-ionized) water was used in all experiments.

2.2 Methods

2.2.1 Synthesis of PANi

By using oxidative polymerization, PANi was chemically synthesized at room temperature. Ammonium persulfate ((NH₄)₂S₂O₈) (45.34 gm) was dissolved in doubly distilled water (100 ml) and mixed with magnetic stirring for 90 min. Again, with constant stirring for 90 min, aniline monomer (18 ml, for better yield) was added drop by drop from a burette, in an ammonium persulfate solution. The resultant product appears greenish black and was kept for 12 h at room temperature. To wash the product, 1M hydrochloric acid solution was used. The product was filtered and washed until the filtrate become colorless, and then dried at 45 °C overnight (Ibrahim, 2017).

2.2.2 Synthesis of NaO₂

The sodium superoxide (NaO₂) was prepared using spray pyrolysis in an oxygen rich environment at a temperature of 673 K. Sodium nitrate and hydrogen peroxide were used as precursors in the preparation of NaO₂. The suspension for spray pyrolysis was prepared by adding 1 M sodium nitrate in 20 ml H₂O₂ under strong magnetic stirring. Subsequently, this suspension was employed for spraying under constant oxygen flow on SiO₂ heating substrate. The structure and phase purity of NaO₂ were confirmed through XRD analysis that was published in our previous work (Barde, 2016).

2.2.3 Preparation of PANi/NaO₂ composites

The PANi/NaO₂ composites were synthesized in organic medium for good dispersion of NaO₂ in the polymeric matrix, using an ex-situ technique with the quantity of NaO₂ varied in 5 wt.% steps in the range from 5 to 20 wt.%. The composites were labeled for pure PANi as (P₀), 5 wt.% NaO₂ as (P₁), 10 wt.% NaO₂ as (P₂), 15 wt.% NaO₂ as (P₃) and 20 wt.% NaO₂ as (P₄). The samples were subjected to an optical study using ultraviolet–visible spectro-photometer on samples of equal thickness (2 ± 0.1 mm) to record the optical properties of all prepared composites. The samples were also tested by XRD, SEM and FTIR as published in our previous work (Barde, 2016).

3. Results and Discussion

The optical absorption spectrum allows estimating the optical energy band gap of crystalline and amorphous materials. The absorption corresponds to electron excitation from the valance band to the conduction band, and is used to verify the character and value of the optical band gap (Cabuk, & Gunduz, 2017). The absorption spectra of PANi/NaO₂ composites were obtained over the range 200-700 nm. The absorption coefficient (α) was calculated using (Fox, 2001):

$$\alpha(\vartheta) = \frac{2.303 A}{l}$$

where l is the sample thickness in cm and A is defined by $A = \log(I_0/I)$ where I_0 is the intensity of the incident beam and I is the intensity of transmitted beam.

Figure 1 shows a penetrating absorption dip in the region from 210 to 220 nm and a broad hump in the region 300–600 nm. The absorption bands in the regions 200–400 nm and 400–600 nm are attributed to the ligand-to-metal charge transfer (Lian *et al.*, 2009; Li *et al.*, 2008) and to the pair excitation processes (Wang *et al.*, 2014) respectively. The wide absorption band in 250-600 nm may be a charge transfer transition from O₂⁻ to Na⁺ in NaO₂.

The refractive index (n) is another significant parameter in opto-electronic parameters. Refractive index (n) and extinction coefficient (k) are the real and imaginary components of the complex refractive index $N=n-ik$. These components represent the optical properties of the prepared composites. The refractive index has a substantial role in optical communication as well in designing antireflection coatings (Chopra, & Kaur, 1969). The refractive index is calculated by using the relation:

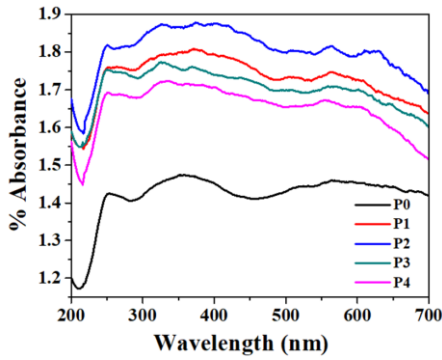


Figure 1. Absorption spectra of pure PANi and PANi/ NaO₂ composites

$$n = \frac{1}{\%T} + \sqrt{\frac{1}{\%T} - 1}$$

where % T is transmission through the sample.

Figure 2 shows the plot of refractive index vs wavelength. Due to the intense absorption by composites in the ultraviolet region, there is a sharp decrease in refractive index around 215 nm. Also, on the lower wavelength side the PANi/ NaO₂ composites have a low refractive index, whereas its value increases up to 370 nm, and beyond this decreases gradually. Initially, the refractive index also increases for 5 and 10 wt. % NaO₂, and then decreases possibly due to non-bridging oxygen (NBO) atoms. The composites with 10 wt. % NaO₂ show the largest refractive index.

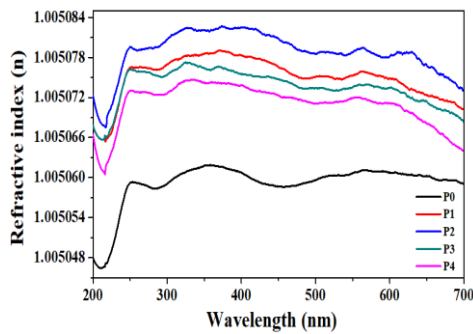


Figure 2. Variation of the refractive index as a function of wavelength

Extinction coefficient can be estimated by (Gedia *et al.*, 2015)

$$k = \frac{\alpha\lambda}{4\pi}$$

where α is % absorption and λ is the wavelength.

Figure 3 shows that beyond the wavelength 225 nm, the extinction coefficient of undoped PANi and all PANi/ NaO₂ composites increases linearly, indicating light trapping. From this, we conclude that light trapping is proportional to wavelength (Barde, 2016; Barde, Nemade, & Waghuley, 2015). On other hand, the wavelengths between 200 and 225 nm are not trapped by the samples as the extinction coefficient is nearly constant between 200 and 225 nm. The largest extinction coefficient was found for the 10 wt. % case of PANi/NaO₂ composite.

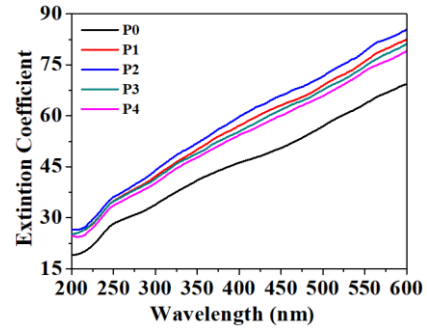


Figure 3. Variation of extinction coefficient as a function of wavelength

Analysis of absorption spectra is the most valuable means for explaining the optical transition and electronic band structure of materials. The band gap is also a very important property for photovoltaic device applications. The basic principle is that an electromagnetic wave interacts with the electron in the valance band and a photon having higher energy than the band gap will be absorbed as the electron is transferred across the fundamental gap to the conduction band. The expression of the absorption coefficient, (α), to determine direct band gap (E_g) was given by (Song, Wang, Yuan, Yao, & Jing, 2015):

$$\alpha h\nu = A(h\nu - E_g)^m$$

where A is an energy dependent constant, E_g is the band gap of the material, and the index m is a constant with discrete values 1/2, 3/2, 2 or more, depending on whether the transition is direct or indirect and allowed or forbidden, respectively (Shumaila *et al.*, (2011)).

Figure 4 shows the Tauc plots between $(\alpha h\nu)^2$ and $h\nu$ for all compositions of PANi/NaO₂ composites. By extrapolation of the linear part of the plot, the band gap energy was estimated. It was found that on increasing NaO₂, E_g decreased from 2.538 to 2.307 eV and became narrower. The doping of NaO₂ may increase localized electrons due to an increase of the donor centers, which decreases the band gap, and this is responsible for the red shift of the absorption edge (Shailajha, Geetha, Vasantharani, & Sheik Abdul Kadhar, 2015). This band gap narrowing is predictable and important to applications in photocatalysis.

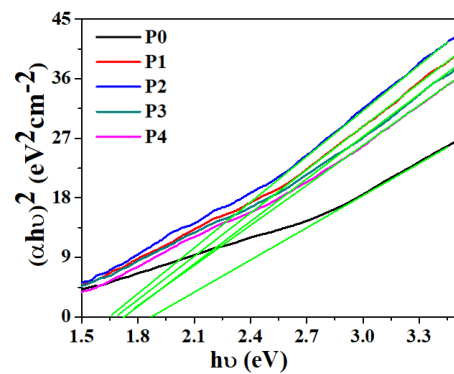


Figure 4. Tauc plot of $(\alpha h\nu)^2$ versus photon energy.

The dielectric function comprises (i) its real part (ϵ_r), which signifies the capability of materials to decrease the speed of light; and (ii) its imaginary part (ϵ_i), which represents absorption of energy from an electric field due to dipole motion. Both these parts have direct relations with refractive index and extinction coefficient (Equations (3) and (4)) (Abdullah, 2013; Barde, Nemade, & Waghuley, 2015).

$$\epsilon_r = n^2 - k^2$$

$$\epsilon_i = 2nk$$

where k is the extinction coefficient and n the refractive index.

It was found that the real dielectric constant (ϵ_r) mostly depended on refractive index (n^2) because of low values of extinction coefficient (k), while the imaginary dielectric constant (ϵ_i) mostly depended on extinction coefficient (k) which is related to the variation of absorption coefficient. Figure 5 shows the variation of the real dielectric constant with wavelength. The real dielectric constant increased linearly with wavelength. The 10 wt. % of NaO_2 sample shows the largest real dielectric constant, hence this sample exhibits the highest ability to slow down light (Sharma, & Katyal, 2007).

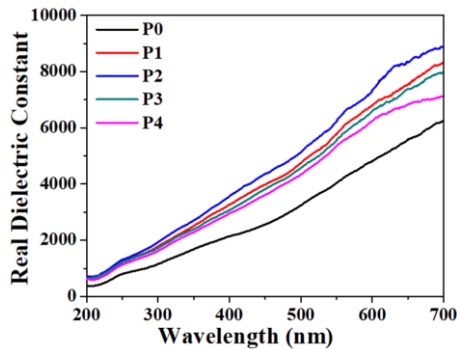


Figure 5. Variation of real dielectric constant

The plots of the imaginary dielectric constant against wavelength are shown in Figure 6. The imaginary dielectric constant increased linearly with wavelength, and the 10 wt. % case of NaO_2 in sample had the largest energy absorption from an electric field due to dipole motion (Bakr *et al.*, 2011). Both the real and imaginary parts show the same pattern and the real dielectric constant was larger than the imaginary dielectric constant.

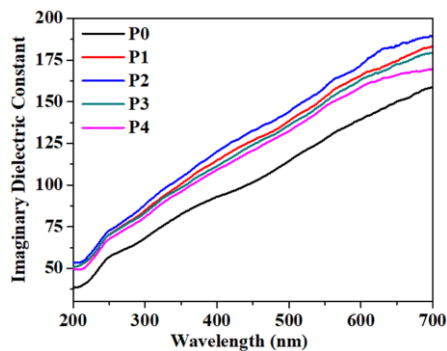


Figure 6. Variation of imaginary dielectric constant.

Optical response is explained by optical conductivity (σ_{opt}) and its dimension is similar to frequency, which is valid only in a Gaussian system of units. It is calculated by using following relation (Barde, Nemade, & Waghuley, 2015),

$$\sigma_{opt} = \frac{\alpha cn}{4\pi}$$

where c is velocity of light, α is absorption coefficient, and n the refractive index.

The plot of σ_{opt} versus $h\nu$ is shown in Figure 7. In it σ_{opt} increased with photon energy. Initially as NaO_2 content increases, the optical conductivity first increases and then decreases. The increase in optical conductivity is due to increases in both absorption coefficient and refractive index with NaO_2 , and may be due to the change in density of localized states in the band gap (Yakuphanoglu, Cukurovali, & Yilmaz, 2005) and also may be due to the electron excitation by photon energy.

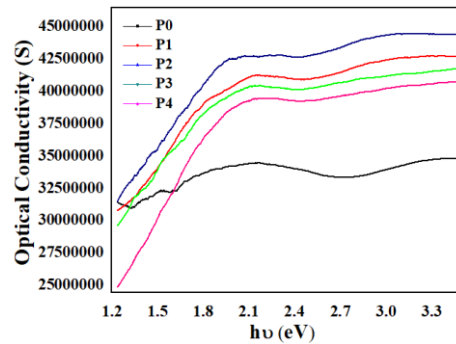


Figure 7. Variation of optical conductivity as a function of photon energy

The optical study of Sodium Superoxide Loaded Polyaniline composites indicates that this material system potentially has applications in terahertz devices, flexible and thin screens, electromagnetic shielding, and electronic components. The characteristics, such as being lightweight, resistant, and stable, enable these composites to be used in electromagnetic shielding applications. Easy control of the electrical conductivity of these composites makes them an important research domain for reliable industrial development.

In the context of environmental impact, polyaniline-based composites exhibit high water dispersibility. In addition to this, polyaniline is considered most promising due to its easy synthesis, environmental stability, low toxicity, and thermal and radiation stability.

4. Conclusions

This work successfully demonstrated PANi/ NaO_2 composites prepared by using an ex-situ technique. The NaO_2 was prepared in a single step by heating sodium nitrate in an oxygen rich environment. The optical absorption spectra of PANi/ NaO_2 composites show an intense absorption dip in the region from 210 to 220 nm and a broad hump in the region 300–700 nm. The prepared composites show trapping of light with extinction coefficient proportional to wavelength. These composites have a low refractive index on the shorter

wavelength side, whereas on the longer wavelength side it increases up to 360 nm; and beyond this the refractive index decreases gradually. The direct band gap was estimated for sodium superoxide loaded polyaniline composites. The dielectric constant measurements show linear behavior as a function of wavelength. Optical conductivity increases with an increase of photon energy due to the change in density of localized states in the band gap.

Acknowledgements

The author acknowledges Director, Govt. Vidarbha Institute of Science and Humanities, Amravati, Head, Department of Physics, Govt. Vidarbha Institute of Science and Humanities, Amravati, and Head, Department of Physics, Sant Gadge Baba Amravati University, Amravati for providing necessary facilities for the work.

References

- Abdullah, A. Q. (2013). Surface and volume energy loss, optical conductivity of rhodamine 6G dye (R6G). *Chemistry and Materials Research*, 3(10), 56-63.
- Bakr, N. A., Funde, A. M., Waman, V. S., Kamble, M. M., Hawaldar, R. R., Amalnerkar, D. P., & Jadkar, S. R. (2011). Determination of the optical parameters of a-Si: H thin films deposited by hot wire-chemical vapour deposition technique using transmission spectrum only. *Pramana Journal of Physics*, 76, 519-531.
- Barde, R. V. (2016). Influence of CeO₂ content on complex optical parameters of phosphovanadate glass system. *Spectrochimica Acta, part A: Molecular and Biomolecular Spectroscopy*, 153, 160-164.
- Barde, R. V. (2016). Preparation, characterization and CO₂ gas sensitivity of polyaniline doped with sodium superoxide (NaO₂). *Material Research Bulletin*, 73, 70-76.
- Barde, R. V., Nemade, K. R., & Waghuley, S. A. (2015). Complex optical study of V₂O₅-P₂O₅-B₂O₃-Dy₂O₃ glass systems. *Journal of Taibah University for Science's*, 10(3), 340-344.
- Barde, R. V., Nemade, K. R., & Waghuley, S. A. (2015). Complex optical study of V₂O₅-P₂O₅-B₂O₃-GO glass systems by ultraviolet-visible spectroscopy. *Optical Materials*, 40, 118-121.
- Cabuka, M., & Gunduz B. (2017). Controlling the optical properties of polyaniline doped by boric acid particles by changing their doping agent and initiator concentration. *Applied Surface Science*, 424(3), 345-351
- Chen, C. H. (2003). Thermal and morphological studies of chemically prepared emeraldine-base-form polyaniline powder. *Journal of Applied Polymer Science*, 89, 2142-2148.
- Chopra, K. L., & Kaur, I. (1969). Thin film phenomena. New York, NY: McGraw-Hill.
- Fox, M. (2001). Optical properties of solids. New York, NY: Oxford University Press.
- Gedia, S., Reddy, V., Reddy, M., Parkb, C., Wookb, J. C., & Reddy, K. T. R. (2015). Comprehensive optical studies on SnS layers synthesized by chemical bath deposition. *Optical Materials*, 42, 468-475.
- Hartmann, P., Bender, C. L., Vracar, M., Garsuch, A., Durr, A. K., Janek, J., & Adelhelm, P. (2013). Rechargeable room-temperature sodium superoxide (NaO₂) battery. *Nature Materials*, 12, 228-232.
- He, M., Lau, K. C., Ren, X., Xiao, N., McCulloch, W. D., Curtiss, L. A., & Wu, Y. (2016). Concentrated electrolyte for the sodium-oxygen battery: Solvation structure and improved cycle life. *Angewandte Chemie International Edition*, 55, 1-6.
- Ibrahim K. A. (2017). Synthesis and characterization of polyaniline and poly (aniline-co-o-nitroaniline) using vibrational spectroscopy. *Arabian Journal of Chemistry*, 10, S2668-S2674
- Khairy, M., & Gouda, M. E. (2015). Electrical and optical properties of nickel ferrite/polyaniline nano composite. *Journal of Advanced Research*, 6, 555-562.
- Li, F., Wei, Z., Manthiram, A., Feng, Y., Maa, J., & Maid, L. (2019). Sodium-based batteries: From critical materials to battery systems. *Journal of Materials Chemistry A*, 7, 9406-9431.
- Li, X. G., Li, A., & Huang, M. R. (2008). Facile high-yield synthesis of polyaniline nanosticks with intrinsic stability and electrical conductivity. *Chemistry - A European Journal*, 14(33), 10309-10317.
- Lian, J. B., Duan, X. C., Ma, J. M., Peng, P., Kim, T., & Zheng, W. J. (2009). Hematite (alpha-Fe₂O₃) with various morphologies: ionic liquid-assisted synthesis, formation mechanism, and properties. *ACS Nano*, 3(11), 3749-3761.
- Mathew, R. J., Yang, D. L., & Mattes, B. R. (2002). Effect of elevated temperature on the reactivity and structure of polyaniline. *Macromolecules*, 35, 7575-81.
- Mini, V., Archana, K., Raghu, S., Sharanappa, C., & Devendrappa, H. (2016). Nanostructured multifunctional core/shell ternary composite of polyaniline-chitosan-cobalt oxide: preparation, electrical and optical properties. *Materials Chemistry and Physics*, 170, 90-98.
- Park, H., Kim, J., Lee, M. H., Park, S. K., Do-Hoon Kim, Bae, Y., . . . Kang, K. (2018). Highly durable and stable sodium superoxide in concentrated electrolytes for sodium-oxygen batteries. *Advanced Energy Materials*, 8(34), 1801760.
- Peled, E., Golodnitsky, D., Mazor, H., Goor, M., & Avshalomov, S. (2011). Parameter analysis of a practical lithium- and sodium-air electric vehicle battery. *Journal of Power Sources*, 196(16), 6835-6840.
- Ren, X., & Wu, Y. (2013). A low-overpotential potassium-oxygen battery based on potassium superoxide. *Journal of the American Chemical Society*, 135(8), 2923-2926.

- Shailajha, S., Geetha, K., Vasantharani, P., & Sheik Abdul Kadhar, S. P. (2015). Effects of copper on the preparation and characterization of Na–Ca–P borate glasses. *Spectrochimica Acta Part A: Molecular and Biomolecular Spectroscopy*, 138, 846–856.
- Sharma, P., & Katyal, S. C. (2007). Determination of optical parameters of a-(As₂Se₃)₉₀Ge₁₀ thin film. *Journal of Physics D: Applied Physics*, 40, 2115–2120.
- Shumaila, Lakshmi, G. B. V. S., Alam, M., Siddiqui, A. M., Zulfequar, M., & Husain, M. (2011). Synthesis and characterization of Se doped polyaniline. *Current Applied Physics*, 11, 217–222.
- Song, S., Wang, Y., Yuan, X., Yao, W., & Jing, W. (2015). Characterization and preparation of Sn-doped CuGaS₂ thin films by paste coating. *Materials Letters*, 148, 41–44.
- Stenicka, M., Pavlinek, V., Saha, P., Blinova, N. V., Stejskal, J., & Quadrat, O. (2008). Conductivity of flowing polyaniline suspensions in electric field. *Colloid and Polymer Science*, 286, 1403–1409.
- Vadukumpully, S., Paul, J., Mahanta, N., & Valiyaveetil, S. (2011). Flexible conductive graphene/polyvinyl chloride) composite thin films with high mechanical strength and thermal stability. *Carbon*, 49, 198–205.
- Wang, T., Zhou, S., Zhang, C., Lian, J., Liang Y., & Yuan, W. (2014). Facile synthesis of hematite nanoparticles and nanocubes and their shape-dependent optical properties. *Journal of Chemistry*, 38, 46–49.
- Xu, X., Hui, K. S., Dinh, D. A., Hui, K.N., & Wang, H. (2019). Recent advances in hybrid sodium-air batteries. *Materials Horizons*, 6, 1306–1335.
- Yakuphanoglu, F., Cukurovali, A., & Yilmaz, I. (2005). Refractive index and optical absorption properties of the complexes of a cyclobutane containing thiazolyldiazone ligand. *Optical Materials*, 27, 1363–1368.
- Yilmaz, K., Akgoz, A., Cabuk, M., & Karaagac, H. (2011). Electrical transport, optical and thermal properties of polyaniline-pumice composites. *Materials Chemistry and Physics*, 130, 956–961